ChemComm

Accepted Manuscript

ChemComm

COMMUNICATION

The Promotion Effect of Isolated Potassium Atoms with Hybridized Orbitals in Catalytic Oxidations†

Fei Xu,[a] Zhiwei Huang,[a] Pingping Hu,[a] Yaxin Chen,[a] Lei Zheng,[b] Jiayi Gao[a] and Xingfu Tang*[a]

The nature of the promotion effect of isolated potassium atoms anchored on surfaces of a Hollandite manganese oxide was investigated by studying their geometric and electronic structures. The results reveal that the surface isolated potassium atoms with hybridized *d-sp* orbitals specifically promote oxygen activation, so enhancing the low-temperature reactivity in catalytic oxidation.

The promotion effect of alkali metals in heterogeneous catalysis has been intensively studied in the past few decades, because alkali promoters such as potassium give rise to the positive effects on many important catalytic reactions.[1] Two representative cases about potassium promoter are the synthesis of ammonia and the Fischer-Tropsch reaction over iron-based catalysts. In the ammonia synthesis, potassium promoter enhances the rate of N_2 dissociation on the metallic iron surfaces by 2-3 orders of magnitude.[2,3] In the Fischer-Tropsch reactions, potassium increases the selectivity of iron-based catalysts.[4] Similar promotion effects of alkali metals have also been reported for oxidation reactions in oxide catalysts.[5] In general, the alkali promotion effect is attributed to the change of the electronic features of active components and adsorbed reactant molecules,[6-9] so enhancing catalytic performance. However, few studies concern the geometric and electronic structures of the alkali promoters themselves due to their relatively "simple" electron orbital structures and easy mobility during catalytic reactions.[10] As a matter of fact, these structure features should be associated with the intrinsic nature of the promotion effect.

Owing to the structural diversity and surface complexity of alkali metals (salts or oxides), experimental investigations of these characteristics of the promoters remain challenging.[8] As a consequence, the promotion effect including the determination of the geometric and electronic structures of

alkali metals is generally investigated by theoretical studies.[9,11] In water-gas shift reactions, a PtK₆ octahedron with the Pt core was theoretically predicted to be the most promising active structure by the charge transfer from K to Pt, which was favourable for activation of oxygen species.[11] The electron donor effect is commonly regarded to be intimately associated with the outermost orbitals ($4s$ and $4p$) of potassium.[13] Note that the contribution of the K $3p$ orbitals to the electron-donor effect was theoretically predicted by the outer *d-sp* orbital hybridization,[11,13] but the related experimental evidence is lacking.

Herein we investigate the nature of the promotion effect in catalytic oxidation, focusing on the immediate geometric and electronic structures of potassium stably anchored on surfaces of a Hollandite manganese oxide (HMO), and experimentally evidence the *d-sp* orbital hybridization of potassium. First, we use (scanning) transmission electron microscopy (TEM/STEM) to image the isolated potassium atoms on the HMO surfaces and conduct the extended X-ray absorption fine structure (EXAFS) spectra to determine the local geometric structures. Next, the electronic structures of the isolated potassium atoms are studied by using the X-ray absorption near edge structure (XANES) spectroscopy and X-ray photoelectron spectroscopy. Finally, we investigate the promotion effect of potassium in catalytic oxidation together with reaction kinetic studies.

The isolated potassium atoms anchored on the surfaces of the HMO (K_1/HMO) are clearly observed by the TEM from the HMO [001] zone axis, as shown in Fig. 1a. The closest K-K distance on the HMO (001) plane is determined to be ~7.1 Å (Fig. 1b), much longer than the K-K bonds (~4.6 Å) in the bulk potassium. The synchrotron X-ray diffraction (SXRD) pattern and Rietveld refinement analysis of K_1/HMO evidence that the K-K distance along HMO [001] direction is ~5.7 Å, twice of the lattice parameter along the HMO [001] direction according to K atoms and hollow sites with an alternate stacking in the HMO pores (Fig. S1, Tables S1, S2, ESI†).[14] The results are further confirmed by the high-angle annular dark field scanning transmission electron microscopy (HAADF-STEM) with line-scanned energy dispersive X-ray (EDX) spectra (Fig.

[a] Department of Environmental Science and Engineering, Fudan University, 220 Handan Road, Shanghai 200433, China. E-mail: tangxf@fudan.edu.cn
[b] Research & Development Center for Functional Crystals, Institute of Physics, Chinese Academy of Sciences, Beijing 100190, China.
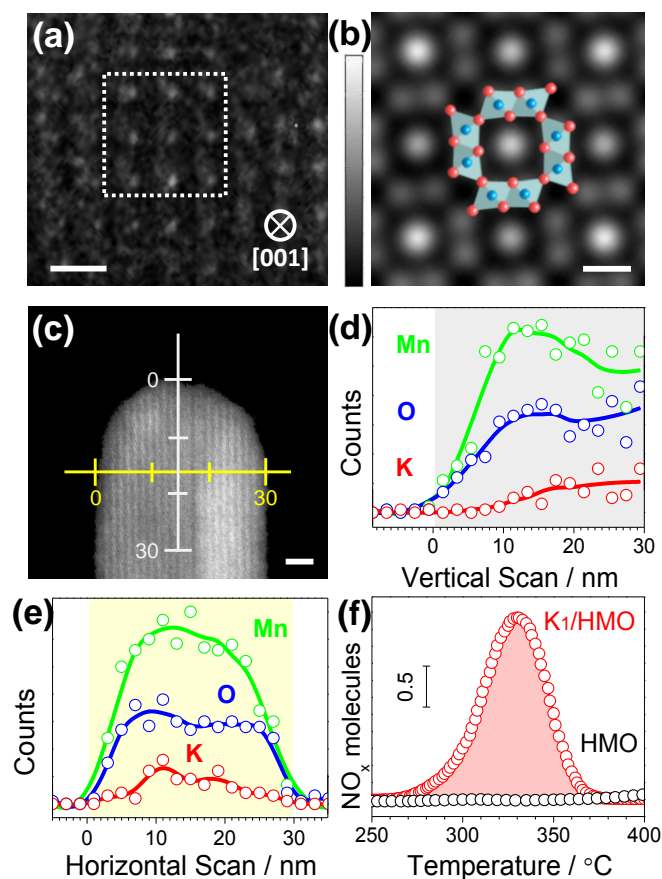
COMMUNICATION

Chemical Communications

Fig. 1 Identification of the isolated potassium atoms anchored on the HMO surfaces. (a) HRTEM image of K_1/HMO viewed from the HMO [001] zone axis. (b) Stimulated HRTEM image in the dot square in (a) with a structural model. The grey, red, and blue balls represent K, O, and Mn atoms, respectively. Blue octahedra are MnO_6. (c) HAADF-STEM image of the K_1/HMO rod with horizontal and vertical line-scanned EDX spectra along the grey line (d) and the yellow line (e), respectively. Scale bar: 1 nm, 0.5 nm and 5 nm in (a), (b) and (c), respectively. (f) NO-TPD profiles of K_1/HMO (red circles) and HMO (black circles) after saturation adsorption of NO at 250 °C, and a red shade represents the desorbed amount of NO_x from K_1/HMO.

Fig. 2 The immediate environments of K atoms in K_1/HMO. FT EXAFS spectra of the K-edge of K_1/HMO with different k^n weight (n = 1, 2, or 3) and KCl with k^2 weight. Inset structural models: a KO_8 polyhedron with a D_{4h} symmetry in K_1/HMO and a KCl_6 octahedron with an O_h symmetry in KCl. The purple, red, and green balls represent K, O and Cl, respectively.

1c-e). Hence, the results demonstrate the presence of the isolated individual potassium atoms.

To substantiate the presence of surface potassium atoms, we use nitric oxide (NO) as a sensitive probing molecule by a temperature-programmed desorption (TPD) procedure (NO-TPD) for K_1/HMO and HMO after saturation adsorption of NO in the presence of O_2 at 250 °C. According to the NO-TPD profiles in Fig. 1f, it is convincing that the NO_x molecules desorbed from K_1/HMO originate from nitrate/nitrite oxides adsorbed on the surface potassium atoms,[15-17] because the desorption amount of NO_x on the potassium-free HMO can be ignored under the identical conditions. These results combined with the electron micrographs above strongly evidence the presence of the isolated potassium atoms on the HMO surfaces.

The local geometric structures of the isolated potassium atoms are investigated by using the EXAFS spectroscopy and the SXRD measurement. Fig. 2 displays the Fourier transform (FT) amplitudes of the EXAFS spectra at the K K-edge of K_1/HMO with different k^n weights (n = 1, 2 or 3) and KCl wth k^2
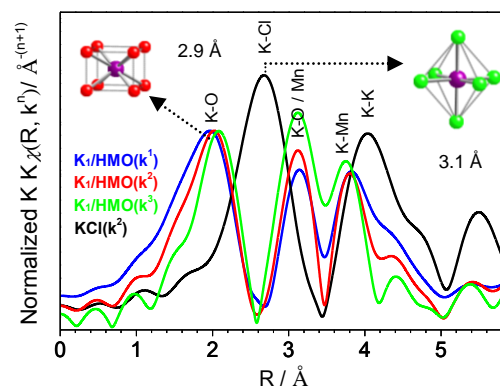
weight. The structural parameters obtained by fitting the spectra with theoretical models are listed in Table S3 (ESI†), and the curve-fitting of R-space, and inverse FT spectra are given in Fig. S2 (ESI†). The local environments of the isolated potassium atoms of K_1/HMO are significantly different from those of KCl judging from their FT spectra (Fig. 2). As expected, the first shell in the FT spectra of KCl represents the K-Cl bond with an average bond length of ~3.1 Å and a coordination number (CN) of six, consistent with a KCl_6 octahedron with an O_h symmetry (Fig. 2, inset). The interatomic distance in the first shell for K_1/HMO can be attributed to the K-O bonds with the bond length of ~2.9 Å and a CN of eight (Table S3, ESI†), and the second shell should be assigned to both the second K-O distance and the near neighbor K-Mn distance according to the different amplitudes with different k weights and the Rietveld SXRD refinement (Table S4, ESI†). The absence of the intensive EXAFS amplitude of the K-K distance indicates the potassium atoms are at the atomically dispersed states. The results are consistent with the Rietveld refinement analysis of the SXRD pattern of K_1/HMO, which gives a coordination configuration of a KO_8 polyhedron with a D_{4h} symmetry (Fig. 2, inset).

The electronic structures of the isolated potassium atoms are studied by using the XANES spectroscopy and the X-ray photoelectron spectroscopy (Fig. 3). The XANES spectrum at the K K-edge of K_1/HMO is distinguished from that of KCl by the presence of a low intensity pre-edge (Fig. 3a, Fig. S3, ESI†).[19] In particular, the $1s \rightarrow 3d$ pre-edge features are sensitive to the coordination geometry of excited atoms.[20] As the octahedral potassium centers in KCl are centro-symmetric without d-p mixing, only rather low intensity pre-edge appears due to the quadrupole transition. The relatively intense pre-edge of the K centers with a pseudo-tetragonal prism structure in K_1/HMO indicates the presence of $1s \rightarrow 3d$ dipole allowed contribution due to 3d-4p mixing, that is, d-sp hybridization. Therefore, the XANES spectrum evidently indicates that the presence of the hybridized d-sp orbitals of potassium atoms, apparently analogue to the outermost orbital hybridization of metal K.[13]
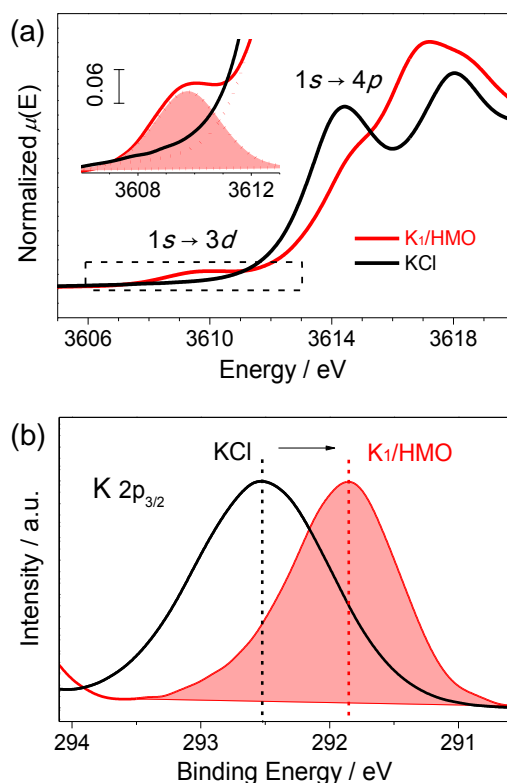
Fig. 3 Electronic structures of the isolated potassium atoms. (a) XANES spectra of K$_1$/HMO and KCl at the K K-edge together with the corresponding pre-edge XANES spectra (inset, and spectral fitting edges are red dotted curves). (b) K 2$p_{3/2}$ XPS of K$_1$/HMO (red curve with the red shade) and KCl (black curve).

The K 2p X-ray photoelectron spectra (XPS) of K$_1$/HMO and KCl are conducted and shown in Fig. 3b (Fig. S4, ESI†). The binding energy (BE) of the K 2p peak shifts down to lower BE by ~0.6 eV for the isolated potassium atoms with respect to that of KCl, from 292.5 eV for KCl to 291.9 eV for K$_1$/HMO. The BE of K 2$p_{3/2}$ for K$_1$/HMO is much lower than that (~293 eV) of K$^+$ in K$_2$O.[21] This indicates that the isolated potassium atoms have higher electron density than K$^+$, coincident with the d-sp orbital hybridization of potassium evidenced by the above XANES spectra. Hence, the isolated potassium atoms with the high electron density should have a much greater promotion effect than K$^+$ in potassium compounds,[13,22] so high catalytic activity in oxidation reactions.

The promotion effect of the isolated potassium atoms is investigated in complete oxidation of formaldehyde (HCHO) and acetate, which are typical air pollutants,[23,24] and contributes greatly to atmospheric particulate emissions, leading to the increase of severe haze events.[25] The conversion of HCHO over K$_1$/HMO and the potassium-free HMO as a function of reaction temperature is shown in Fig. S5 (ESI†), and the temperature-dependent conversion is observed. K$_1$/HMO has the high catalytic activity for complete oxidation of HCHO at low temperatures lower than 100 °C, whereas the potassium-free HMO shows low catalytic activity under the same reaction conditions. The conversion over K$_1$/HMO is 5% at 80 °C, which increases up to 50% at 100 °C. At 120 °C, almost complete oxidation of HCHO into CO$_2$ and H$_2$O can be

achieved over K$_1$/HMO, while the potassium-free HMO only gives less than 50% conversion of HCHO at this temperature. The catalytic activities toward HCHO or acetate oxidation also increase with the amount of potassium, as shown in Fig. S3 (ESI†). Therefore, the surface isolated potassium atoms have the great promotion effect in catalytic oxidation at low temperatures.

The steady-state reaction rates in terms of a turnover frequency (TOF, number of converted HCHO molecules per surface K atoms per second) are shown in an Arrhenius plot (Fig. S5, ESI†) in order to clearly understand the promotion effect of potassium. The pre-exponential factor (F_p) for K$_1$/HMO is 1.0×10^6 s^{-1}, ten times more than the corresponding F_p (9.9×10^4 s^{-1}) for the potassium-free HMO. This suggests that the promotion effect originated from direct bonding between potassium atoms and adsorbed reactant molecules (HCHO and/or O$_2$),[11] leading to the higher reaction rates of K$_1$/HMO than those of the potassium-free HMO in HCHO oxidation.

To shed light on the promotion effect of the isolated potassium atoms on HCHO and/or O$_2$ in the HCHO oxidation, we conduct surface reaction kinetics of the HCHO oxidation at low temperature over K$_1$/HMO and the potassium-free HMO at the conversions less than 20%.[26] As shown in Fig. 4, the reaction order of O$_2$ is 0.9 for K$_1$/HMO, much higher than that (only 0.2) of the potassium-free HMO (Fig. 4a), and the reaction orders of HCHO over both K$_1$/HMO and the
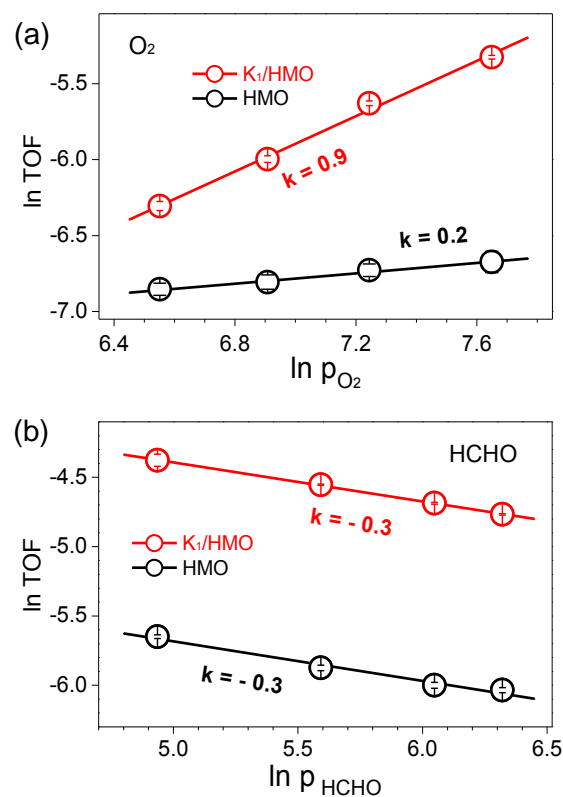

Fig. 4 Reaction kinetics of the catalytic oxidation of HCHO. Reaction orders for O$_2$ (a) and HCHO (b) over K$_1$/HMO and the potassium-free HMO at the reaction temperature of 90 °C. The slope k represents the reaction order.

potassium-free HMO are -0.3 (Fig. 4b), indicative of the high concentration of the adsorbed HCHO species covering the surfaces of both catalysts. The adsorbed HCHO inhibits O_2 activation unless consumed by surface lattice oxygen, generating oxygen defects. The increase of the O_2 concentration decreases the HCHO coverage on the K_1/HMO surface by promoting CO_2 and H_2O formation, leading to an almost first-order dependence on O_2 concentration, while very weak dependency on O_2 concentration over the potassium-free HMO is due largely to the low reaction rates of HCHO oxidation. Reaction kinetics indicates that the surface isolated potassium atoms of K_1/HMO have much stronger activation ability to molecular O_2 than HMO in catalytic oxidation. In fact, the HCHO oxidation in the low-reactivity steady state regime often follows a Mars-van Krevelen mechanism,[27,28] and oxygen activation includes both molecular O_2 and surface lattice oxygen. Hence, the promotion effect of the isolated potassium atoms should cover the activation of molecular O_2 and surface lattice oxygen.

The dissociation step of O_2 is often considered as one of the important rate-limiting steps in catalytic oxidation. The activation of O_2 is intimately associated with the electronic states of potassium. A previous theoretical calculation reported that electron-abundant potassium atoms are energetically favorable for dissociation of O_2 by charge transfer from potassium to antibonding π^* and σ^* orbitals of O_2.[12] As a consequence, the isolated potassium atoms with the high electron density are favorable for promoting O_2 activation. From the kinetic point of view, during such an activation process of O_2, the d-sp hybridization of the isolated potassium atoms plays an important role, and local transfer of sp electrons to empty d shell weakens the Pauli repulsion and allows O_2 molecule to approach and continue into the chemisorption region, and finally leads to O_2 dissociation.[29,30] Therefore, the isolated potassium atoms have the strong promotion effect on oxygen activation in catalytic oxidation.

In conclusion, we investigated the promotion effect of potassium anchored on the HMO surfaces in catalytic oxidation. The HRTEM image, the HAADF-STEM image, and the EXAFS spectra showed that the isolated potassium atoms were anchored on the HMO surfaces to give the geometric configuration of the KO_8 polyhedron with a D_{4h} symmetry. The combination of the XANES spectra and XPS with catalytic reaction kinetics demonstrated that the isolated potassium atoms had the hybridized d-sp orbitals and the high electron density, specifically promoted oxygen activation, and enhanced the low-temperature catalytic reactivity in the complete oxidation of HCHO and acetylate. This finding gives direct evidence for explaining the alkali promotion effect by investigating the geometric and electronic characteristics of alkali metal promoters themselves, and provides a reasonable strategy to develop improved catalysts promoted by alkali metals.

Notes and references

1   W. -D. Mross, *Catal*. *Rev*. *Sci*. *Eng*., 1983, **25**, 591-637.
2   G. Ertl, S. B. Lee and M. Weiss, *Surf*. *Sci*., 1982, **114**, 527-545.
3   A. Nielsen, *Catal*. *Rev*. *Sci*. *Eng*., 1981, **23**, 17-51.
4   K. Herzog and J. Gaube, *J. Catal*., 1989, **115**, 337-346.
5   M. Akimoto and E. Echigoya, *J. Catal*., 1974, **35**, 278-288.
6   T. S. Rahman, S. Stolbov and F. Mehmood, *Appl*. *Phys*. *A*, 2007, **87**, 367-374.
7   S. J. Jenkins and D. A. King, *J. Am*. *Chem*. *Soc*., 2000, **122**, 10610-10614.
8   C. Huo, B. Wu, P. Gao, Y. Yang, Y. Li and H. Jiao, *Angew*. *Chem*. *Int*. *Ed*., 2011, **50**, 7403-7406.
9   Y. Zhai, D. Pierre, R. Si, W. Deng, P. Ferrin, A. U. Nilekar, G. Peng, J. A. Herron, D. C. Bell, H. Saltsburg, M. Mavrikakis and M. Flytzani-Stephanopoulos, *Science*, 2010, **329**, 1633-1636.
10 H. An and P. J. McGinn, *Appl. Catal*. *B*, 2006, **62**, 46-56.
11 Z. Liu and P. Hu, *J. Am*. *Chem*. *Soc*., 2001, **123**, 12596-12604.
12 C. Janiak, R. Hoffmann, P. Sjövall and B. Kasemo, *Langmuir*, 1993, **9**, 3427-3440.
13 L. Pauling, *General Chemistry*, BN Publishing, 2011.
14 M. Pasero, *Rev*. *Mineral*. *Geochem*., 2005, **57**, 291-305.
15 Q. Li, X. Wang, Y. Xin, Z. Zhang, Y. Zhang, C. Hao, M. Meng, L. Zheng and L. Zheng, *Sci*. *Rep*., 2014, **4**, 4725.
16 Z. Huang, X. Gu, W. Wen, P. Hu, M. Makkee, H. Lin, F. Kapteijn and X. Tang, *Angew*. *Chem*. *Int*. *Ed*., 2013, **52**, 660-664.
17 Y. Lee, J. Park, S. Jun, D. Choi and J. Yie, *Carbon*, 2004, **42**, 59-69.
18 J. Vicat, E. Fanchon, P. Strobel and D. T. Qui, *Acta Crystallogr*. *B*, 1986, **42**, 162-167.
19 L. G. Parratt, *Rev*. *Mod*. *Phys*., 1959, **31**, 616-645.
20 S. Bordiga, E. Groppo, G. Agostini, J. A. van Bokhoven and C. Lamberti, *Chem*. *Rev*., 2013, **113**, 1736-1850.
21 R. Sawyer, H. W. Nesbitt and R. A. Secco, *J. Non-Cryst*. *Solids*., 2012, **358**, 290-302.
22 A. Ozaki, K. Aika and Y. Morikawa, *Proc*. *5th Int*. *Congr*. *Catal*., North-Holland, Amsterdam, 1973.
23 M. Lee, B. G. Heikes, D. J. Jacob, G. Sachse and B. Anderson, *J. Geophys*. *Res*., 1997, **102**, 1301-1309.
24 M. Lee, B. G. Heikes and D. J. Jacob, *J. Geophys*. *Res*., 1998, **103**, 13201-13212.
25 R. Huang, Y. Zhang, C. Bozzetti, K. Ho, J. Cao, Y. Han, K. R. Daellenbach, J. G. Slowik, S. M. Platt, F. Canonaco, P. Zotter, R. Wolf, S. M. Pieber, E. A. Bruns, M. Crippa, G. Ciarelli, A. Piazzalunga, M. Schwikowski, G. Abbaszade, J. Schnelle-Kreis, R. Zimmermann, Z. An, S. Szidat, U. Baltensperger, I. E. Haddad and A. S. H. Prévôt, *Nature*, 2014, **514**, 218-222.
26 V. P. Zhdanov and B. Kasemo, *Surf*. *Sci*. *Rep*., 1994, **20**, 113-189.
27 C. F. Mao and M. A. Vannice, *J. Catal*., 1995, **154**, 230-244.
28 Z. Huang, X. Gu, Q. Cao, P. Hu, J. Hao, J. Li and X. Tang, *Angew*. *Chem*. *Int*. *Ed*., 2012, **51**, 4198-4203.
29 J. Harris and S. Andersson, *Phys*. *Rev*. *Lett*., 1985, **55**, 1583-1586.
30 J. E. Post, R. B. Vondreele and P. R. Buseck, *Acta Crystallogr*. *B*, 1982, **38**, 1056-1065.